Article

Large Differences in Secondary Metal#Arene Interactions in the Transition-Metal Dimers ArMMAr (Ar = Terphenyl; M = Cr, Fe, or Co): Implications for Cr#Cr Quintuple Bonding

Giovanni La Macchia, Laura Gagliardi, Philip P. Power, and Marcin Brynda

J. Am. Chem. Soc., **2008**, 130 (15), 5104-5114 • DOI: 10.1021/ja0771890 • Publication Date (Web): 13 March 2008

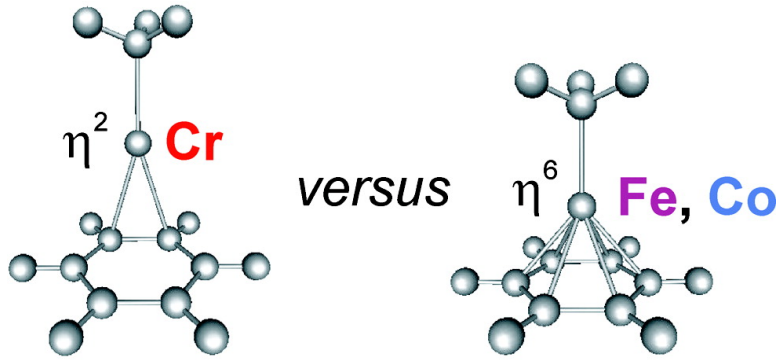

More About This Article

Additional resources and features associated with this article are available within the HTML version:

- Supporting Information
- Links to the 7 articles that cite this article, as of the time of this article download
- Access to high resolution figures
- Links to articles and content related to this article
- Copyright permission to reproduce figures and/or text from this article

View the Full Text HTML

J|A|C|S
ARTICLES

Published on Web 03/13/2008

Large Differences in Secondary Metal−Arene Interactions in the Transition-Metal Dimers ArMMAr (Ar = Terphenyl; M = Cr, Fe, or Co): Implications for Cr−Cr Quintuple Bonding

Giovanni La Macchia, Laura Gagliardi,* Philip P. Power, and Marcin Brynda*

Department of Chemistry, University of California, Davis, One Shields Avenue, Davis, California 95616, and Department of Chemistry, University of Geneva, 30 quai E. Ansermet, Geneva 1211, Switzerland

Received September 17, 2007; E-mail: mabrynda@ucdavis.edu; laura.gagliardi@chiphy.unige.ch

Abstract: Quantum mechanical calculations, using both CASPT2 and DFT methods, for the model systems (MeMMMe, PhMMPh, (MeMMMe)$(C_6H_6)_2$, Ar§MMAr§, Ar#MMAr#; M = Cr, Fe, Co; Ar§ = C_6H_4-2(C_6H_5), Ar# = C_6H_3-2,6(C_6H_3-2,6-Me_2)$_2$) are described. These studies were undertaken to provide a multireference description of the metal−metal bond in the simple dimers MeMMMe and PhMMPh (M = Cr, Fe, Co) and to determine the extent of secondary metal−arene interaction involving the flanking aryl rings of the terphenyl ligands in quintuply bonded Ar′CrCrAr′ (Ar′ = C_6H_3-2,6(C_6H_3-2,6-Pr^i_2)$_2$). We show that in the Cr−Cr species the Cr−arene interaction is a feeble one that causes only a small weakening of the quintuple bond. In sharp contrast, in the analogous Fe and Co species strong η^6-arene interactions that preclude significant metal−metal bonding are predicted.

Introduction

The recent characterization of the quintuply bonded chromium species Ar′CrCrAr′ (Ar′ = C_6H_3-2,6(C_6H_3-2,6-Pr^i_2)$_2$) has raised new bonding questions and stimulated theoretical work on transition-metal species with potentially high metal−metal bond orders.[1−4] The Ar′CrCrAr′ compound featured a short Cr−Cr bond of 1.8351(4) Å as well as a trans-bent, planar C_{ipso}−Cr−Cr−C_{ipso} core structure, Cr−Cr−C = 102.78(1)°. There was also a relatively short (2.294(1) Å) secondary Cr−C interaction involving an ipso-carbon of one of the flanking aryl rings as illustrated in Scheme 1. Earlier calculations[5] by Weinhold and Landis on the simple group 6 model species HWWH predicted that its optimized geometry had indeed a trans-bent (C_{2h}) structure as well as a quintuple W−W bond. These, as well as their more recent studies on the model species MeMMMe (M = Cr, Mo or W), led to the conclusion that the trans-bent structure of the RMMR compounds was a result of s−d hybridization which strengthened the M-M bond.[6]

We also reported calculations performed with the high-level multiconfigurational CASPT2 method on model species PhCr-CrPh. This study yielded structural parameters for the trans-bent configuration, Cr−Cr = 1.752 Å, Cr−Cr−C = 88.4°, that differed significantly from those experimentally observed for Ar′CrCrAr′ (a linear form of PhCrCrPh with Cr−Cr = 1.678 Å was calculated to be 1 kcal mol^{-1} more stable than the trans-bent form).[7] In contrast, the bond length in the dimetal Cr_2 molecule calculated at the same level of theory[8] was found to be in almost exact agreement with the experimental value of 1.679 Å.[9] Thus, the following question arises: to what extent do any additional interactions found in the crystal structure, in particular those pertaining to the large size of the Ar′ substituent and the close secondary Cr-ligand approaches, affect the Cr−Cr bonding?

Since the use of large ligands containing flanking aryl moieties has become now a widely used strategy for the stabilization of dimeric, metal−metal bonded species among the main group and transition elements,[10−12] we thought it

Scheme 1. X-ray Crystal Structure of the Ar′CrCrAr′ Species [a]

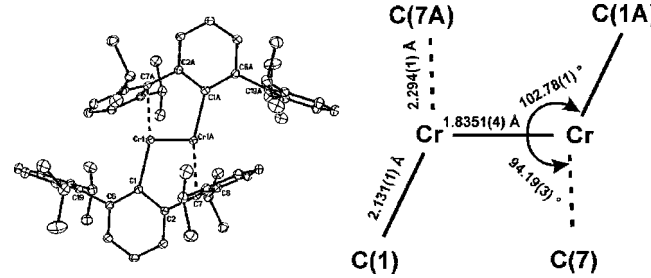

[a] Hydrogens are omitted for clarity with schematic representation of the C_{ipso}−Cr−Cr−C_{ipso} core with relevant structural parameters including Cr−C distances in the secondary interactions with the flanking aryl of the terphenyl ligand.

(1) Nguyen, T.; Sutton, A. D.; Brynda, M.; Fettinger, J. C.; Long, G. J.; Power, P. P. *Science* **2005**, *310*, 844–847.
(2) Frenking, G. *Science* **2005**, *310*, 796.
(3) Radius, U.; Breher, F. *Angew. Chem., Int. Ed.* **2006**, *45*, 3006–3010.
(4) Roos, B. O.; Borin, A. C.; Gagliardi, L. *Angew. Chem., Int. Ed.* **2007**, *46*, 1469–1472.
(5) Weinhold, F.; Landis, C. R. *Chem. Educ.: Res. Pract. Eur.* **2001**, *2*, 91–104.
(6) Landis, C. R.; Weinhold, F. *J. Am. Chem. Soc.* **2006**, *128*, 7335–7345.
(7) Brynda, M.; Gagliardi, L.; Widmark, P.-O.; Power, P. P.; Roos, B. O. *Angew. Chem., Int. Ed.* **2006**, *45*, 3804–3807.
(8) Roos, B. O. *Collect. Czech. Chem. Commun.* **2003**, *68*, 265.
(9) Bondybey, V. E.; English, J. H. *Chem. Phys. Lett.* **1983**, *94*, 443–447.

 10.1021/ja0771890 CCC: $40.75

important to address this topic by quantifying the impact of such weak interactions on the geometry of the CMMC core units for a selection of transition metal dimers—in this case derivatives of Cr, Fe, and Co. We provided a preliminary qualitative report of such interactions in a recent publication,[13] but no quantitative analysis have yet been carried out by theoretical quantum chemistry methods. We restrict our study to the three transition metal dimers and exclude the manganese species since most of the theoretical methods are divided on this very challenging system.[14,15]

The paper is organized as follows: first, we present the theoretical methods used in this study and explain the choice of the model compounds for the metal dimers bearing bulky terphenyl ligands. We begin with the calculations of the energies for various spin multiplicities in the RMMR (R = Me, Ph) model species. Following this, we report the optimized structures of the model species in several spin states and introduce the most important structural features of the computed geometries, briefly discussing the results of torsional potential-energy surface scans that measure the strength of the metal−metal bond and characterize the flatness of the energy surfaces. The second part of the paper includes the results of the optimizations of monomeric ligand–metal/arene species Me−M−Bz, as well as its dimeric analogues, in which the simplest diorgano-dimetal complexes MeMMMe interact with benzene. Calculations on analogous models $Ar^{\S}MMAr^{\S}$ and $Ar^{\#}MMAr^{\#}$ ($Ar^{\S}$ = C_6H_4-2(C_6H_5), $Ar^{\#}$ = C_6H_3-2,6(C_6H_3-2,6-Me_2)$_2$) are also reported, followed by the evaluation of the corresponding bond orders. We then discuss the energetics of the metal-arene interactions in our model species and close with some conclusions.

Computational Methods. Multiconfigurational quantum chemical calculations were performed using the complete active space-SCF (CASSCF)[16] method to generate wave functions for several electronic states of a given symmetry and spin multiplicity. Dynamic correlation was added using second-order perturbation theory, CASPT2.[17] The CASSCF/CASPT2 calculations were performed using the MOLCAS 6.4[18] program package. Scalar relativistic effects were included using the Douglas−Kroll−Hess Hamiltonian[19,20] and the ANO-RCC basis set,[21] where the primitive set 21s15p10d6f4g2 h was contracted to 5s4p2d1f for the transition metals (M), the primitive set 14s9p4d3f2g was contracted to 3s2p1d for carbon, and the primitive set 8s4p3d was contracted to 2s1p for hydrogen. The active space was formed by 14 molecular orbitals (MOs). There are two bonding and two antibonding M−C MOs and five bonding and five antibonding M−M MOs, arising from a linear combination of the M 3d and 4s and the C(methyl/phenyl) radical orbitals. The number of active electrons included in the active space was 14 for the Cr compounds (six from each Cr, corresponding to the valence configuration $3d^5 4s^1$ and one from each C), 18 for the Fe compounds (eight from each Fe, corresponding to the valence configuration $3d^6 4s^2$ and one from each C) and 20 for the Co compounds (nine from each Co, corresponding to the valence configuration $3d^7 4s^2$ and one from each C). In the subsequent CASPT2 calculations the orbitals up to and including the 2p on the transition metals and 1s on C were kept frozen. Calculations on the ground-state of each system and several excited states were performed. Spin–orbit effects were not taken into account, but, according to the results of studies on similar compounds, they do not affect the structure of the ground state.[22] The effective bond order $(EBO)^4$ between the two M atoms was calculated as the sum of the occupation numbers of the bonding orbitals minus the sum of the occupation numbers of the antibonding orbitals, divided by two. DFT optimized geometries were used as starting points and subsequent CASPT2 geometry reoptimization of the most relevant parameters, like the M−M bond distance, M−C bond distance and MMC angle, was performed. Dissociation energies (D_e) have been calculated as energy differences between the energy of the full systems minus twice the energy of half-the systems (at their optimized DFT geometry) with the correction to basis set superposition error (BSSE) using the counterpoise correction. The method has proven to be successful in the study of similar transition-metal compounds, for example, $Re_2Cl_8^{2-}$[23] and $Re_2(CH_3)_8^{2-}$.[24,25]

The investigation of the arene/transition metal interactions was performed with DFT, which is known to reproduce the transition metal–ligands geometries to satisfactory accuracy.[26–35] Since the theoretical analysis of the metal−metal bonds with multiple character (for which the DFT description is known to suffer from its intrinsic monodeterminental character) is not at the focus here, only the quantitative trends in both, M−M bond lengths and the geometries of the CMMC cores induced by the interactions with arene ligands are analyzed. The differences between the noninteracting geometries (MeMMMe) and the geometries of the (MeMMMe)(C_6H_6)$_2$ models are then mapped on the geometrical features obtained from the CASPT2 calculations and finally compared to the experimental geometries. This

(10) (a) Clyburne, J. A. C.; McMullen, N. *Coord. Chem. Rev.* **2000**, *210*, 73–99. (b) Twamley, B.; Haubrich, S. T.; Power, P. P. *Adv. Organomet. Chem.* **1999**, *44*, 1–65.
(11) Power, P. P. *Organometallics* **2007**, *26*, 4362–4372.
(12) Robinson, G. H. *Organometallics* **2007**, *26*, 2–11.
(13) Nguyen, T.; Panda, A.; Olmstead, M. M.; Richards, A. F.; Stender, M.; Brynda, M.; Power, P. P. *J. Am. Chem. Soc.* **2005**, *127*, 8545–8552.
(14) Valiev, M.; Bylaska, E. J.; Weare, J. H. *J. Chem. Phys.* **2003**, *119*, 5955–5964.
(15) Yanagisawa, S.; Tsuneda, T.; Hirao, K. *J. Chem. Phys.* **2000**, *112*, 545–553.
(16) Roos, B. O. In *Advances in Chemical Physics: Ab Initio Methods in Quantum Chemistry-II*; Lawley, K. P., Ed.; John Wiley & Sons Ltd.: Chichester, England, 1987; p 399.
(17) Andersson, K.; Malmqvist, P. A.; Roos, B. O.; Sadlej, A. J.; Wolinski, K. *J. Phys. Chem.* **1990**, *94*, 5483–5488.
(18) Karlströem, G.; Lindh, R.; Malmqvist, P.-A.; Roos, B. O.; Ryde, U.; Veryazov, V.; Widmark, P.-O.; Cossi, M.; Schimmelpfennig, B.; Neogrady, P.; Seijo, L. *Comput. Mater. Sci.* **2003**, *28*, 222–239.
(19) Kroll, N. M. *Phys. Rev. A* **1974**, *82*, 89–155.
(20) Hess, B. A. *Phys. Rev. A* **1986**, *33*, 3742–3748.
(21) Roos, B. O.; Lindh, R.; Malmqvist, P.-A.; Veryazov, V.; Widmark, P.-O. *J. Phys. Chem. A* **2005**, *109*, 6575–6579.
(22) La Macchia, G.; Brynda, M.; Gagliardi, L. *Angew. Chem., Int. Ed.* **2006**, *45*, 6210–6213.
(23) Gagliardi, L.; Roos, B. O. *Inorg. Chem.* **2003**, *42*, 1599–1603.
(24) Ferrante, F.; Gagliardi, L.; Bursten, B. E.; Sattelberger, A. P. *Inorg. Chem.* **2005**, *44*, 8476–8480.
(25) Gagliardi, L. *Theor. Chem. Acc.* **2006**, *116*, 307–315.
(26) Frenking, G.; Sola, M.; Vyboishchikov, S. F. *J. Organomet. Chem.* **2005**, *690*, 6178–6204.
(27) Frenking, G.; Wichmann, K.; Frohlich, N.; Loschen, C.; Lein, M.; Frunzke, J.; Rayon, V. M. *Coord. Chem. Rev.* **2003**, *238–239*, 55–82.
(28) Bencini, A.; Carbonera, C.; Dei, A.; Vaz, M. G. F. *Dalton Trans.* **2003**, 1701–1706.
(29) Dietz, O.; Rayon, V. M.; Frenking, G. *Inorg. Chem.* **2003**, *42*, 4977–4984.
(30) Atanasov, M.; Daul, C. A. *Chem. Phys. Lett.* **2003**, *379*, 209–215.
(31) Goh, S.-K.; Marynick, D. S. *J. Comput. Chem.* **2001**, *22*, 1881–1886.
(32) Frenking, G.; Froehlich, N. *Chem. Rev.* **2000**, *100*, 717–774.
(33) Frohlich, N.; Frenking, G. *Phys. Organomet. Chem.* **1999**, *2*, 173–226.
(34) Creve, S.; Pierloot, K.; Nguyen, M. T. *Chem. Phys. Lett.* **1998**, *285*, 429–437.
(35) Abashkin, Y. G.; Burt, S. K.; Collins, J. R.; Cachau, R. E.; Russo, N.; Erickson, J. W. *NATO ASI Ser., Ser. C* **1996**, *474*, 1–22.

methodology proved to be successful in our recent description of the quintuple character of the Cr−Cr bond in Ar′CrCrAr′.[7] The DFT calculations were performed at both scalar relativistic and nonrelativistic level of theory. The relativistic effects were included using the zero order relativistic approximation (ZORA) relativistic Hamiltonian,[36] which treats the core–electrons explicitly, as implemented in ADF program.[37] In this case the ZORA Hamiltonian was combined with Kohn–Sham formalism using BLYP functional and Slater type of orbitals of triple-ζ quality with one polarization function (TZP). Throughout the text, this implementation is labeled as BLYP/ZORA/TZP. Optimizations of the model molecules with the Ar# ligands (Ar# = C_6H_3-2,6-(C_6H_3-2,6-Me_2)) were performed using BLYP/ZORA combined with TZP basis set for the metal centers and DZP basis set for C and H atoms. The nonrelativistic calculations were carried out using the Gaussian 03 program[38] with the Ahlrichs all electron basis set of double-ζ quality augmented with polarization functions[39] combined with B3LYP functional (this level of theory is hereafter reported as B3LYP/pVDZ). The binding energies form B3LYP/pVDZ calculations were corrected for basis set superposition error (BSSE) using the counterpoise method of Boys and Bernardi.[40] The graphical representations of the optimized structures were generated with GOpenMol software.

Model. The complexity of the terphenyl ligands makes the use of multireference methods for the study of the complete Ar′MMAr′ (Ar′ = C_6H_3-2,6(C_6H_3-2,6-Pr^i_2)$_2$) dimers difficult. Even with use of the monodeterminental DFT methods, it is not trivial to deal with the weak interactions in molecules of such size at a satisfactory theoretical level. The difficulty in describing the secondary intramolecular interactions[41] occurring between covalently bonded fragments lies in the fact that, in order to quantify the fragment−fragment interaction based on the calculated energies, one has to "divide" the molecule into separate subunits, so that the bonding energies between different fragments can be easily computed. To overcome these difficulties, we decided to conduct our theoretical studies on simplified species: benzene-MeMMMe-benzene hereafter abbreviated (MeMMMe)(C_6H_6)$_2$. In these models, the MeMMMe fragment mimics the metal−metal core (C_{ipso}−M−M−C_{ipso}) found in the Ar′MMAr′ dimers, whereas the nearby two flanking aryl of the ligand are modeled by two surrounding benzene molecules. The geometry of the two benzenes was kept frozen during the geometry optimization of the central MeMMMe fragment, and the C_6H_6−C_6H_6 separation (centroid−centroid distance and mutual orientation) was based on the analogous flanking aryl−flanking aryl distance from the X-ray crystallographic files.[42] For the MeMMMe models two possible geometries are involved because of the methyl C_3 symmetry axis: C_{2h} where the distance between the two methyl protons in the symmetry plane remain minimal, and C_{2h}' where this distance is maximized. The (MeMMMe)(C_6H_6)$_2$ molecules were also optimized within C_{2h} and C_{2h}' symmetries (the MeMMMe fragment is constrained into the symmetry plane containing the two opposite carbon atoms of each benzene molecule). The differences between the optimized structures in both symmetries are very small, and we focus mainly of the C_{2h}' symmetry, since this minimizes the steric constraints between the benzenic protons and the proton of the MeMMMe methyl groups in our (MeMMMe)(C_6H_6)$_2$ molecules; in addition, it reflects the situation found in the ArMMAr molecules the most closely. We are of course aware of the fact that this is a rather important simplification and some of its weaknesses are discussed later in the paper. However, it offers the advantage of dealing with a model system containing well-defined fragments. Our initial attempts to use a similar model system containing two benzene molecules, in which the C−M−M−C_{ipso} core was represented by the phenyl−M−M−phenyl (PhMMPh) core remained unsuccessful due to unrealistic sterical constraints between the two benzene molecules and the phenyl groups. For comparison, we also present analogous results on two models mimicking simplified bulky aryls ligands: Ar§MMAr§ (Ar§ = C_6H_4-2(C_6H_5) and Ar#MMAr# (Ar# = C_6H_3-2,6(C_6H_3-2,6-Me_2)$_2$).

Table 1. CASPT2 M−M, C−M Bond Distances (Å), C−M−M and C−M−M−C angles (deg), Dissociation Energies (kcal mol^{-1}), and M−M effective bond orders (EBO) for RMMR species (R = Me, Ph; M = Cr, Fe, Co)

model species	M−M (Å)	C−M (Å)	C−M−M (deg)	C−M−M−C (deg)	EBO	D_e
MeCrCrMe, ^1A_g	1.849	2.100	82.2	180.0	2.96	48
PhCrCrPh[7], ^1A_g	1.752	2.018	88.4	180.0	3.52	76
Ar′CrCrAr′[1], ^1A	1.836[a]	2.132[a]	102.8[a]	180.0[a]	3.43	
MeFeFeMe, ^7A_u	1.989	1.955	129.6	180.0		30
PhFeFePh, ^7A_u	1.970	2.017	79.2	180.0	1.47	36
Ar′FeFeAr′	2.519[a]	2.016[a]	100.4[a]	159.6[a]		
MeCoCoMe, ^5B_u	1.948	1.844	124.3	180.0		42
PhCoCoPh, ^5B_g	1.940	1.926	76.4	180.0	1.38	61
Ar′CoCoAr′, ^5A	2.801[a]	2.019[a]	94.1[a]	163.5[a]	0	

[a] The coordinates and the corresponding bond lengths and bond angles of the Ar′CrCrAr′, Ar′CoCoAr′, and Ar′FeFeAr′ structures (Ar′ = C_6H_3-2,6(C_6H_3-2,6-Pr^i_2)$_2$) are taken from experimental X-ray crystallographic data[42]

Results

Geometries of the RMMR Models (R = Me, Ph; M = Cr, Fe, Co) Obtained from CASSCF/CASPT2 and DFT Calculations. The CASSCF/CASPT2 calculations performed on the MeMMMe and PhMMPh models in their ground-state yielded the structural parameters reported in Table 1. Additional calculations were also performed on some excited states. We shall report here only some of these results. In the MeFeFeMe case, for example, a ^5B_g state lies 9.3 kcal mol^{-1} higher in energy than the ^7A_u ground state. Two other quintet states, ^5A_u, ^5A_g, lie 19.3 and 21 kcal mol^{-1} higher than the septet. Energetically distant septet states were found to be 28.7 kcal mol^{-1} higher in energy than the ground state. In the MeCoCoMe case, the first excited state, a ^5A_g state, lies 4.8 kcal mol^{-1} higher than the ^5B_u ground state and the next quintet state lies 11.2 kcal mol^{-1} higher than the ground state. We will not discuss the excited states further, but instead, focus on the ground state

(36) van Lenthe, E.; Baerends, E. J.; Snijders, J. G. *J. Chem. Phys.* **1994**, *101*, 9783–9792.
(37) ADF ADF 2002. 03, SCM, Theoretical Chemistry, Vrije Universiteit, Amsterdam, The Netherlands, http://www.scm.com.
(38) Frisch, M. J.; *et al*. *Gaussian 03*, revision A.1; Gaussian, Inc.: Pittsburgh, PA, 2003.
(39) Schafer, A.; Horn, H.; Ahlrichs, R. *J. Chem. Phys.* **1992**, *9*, 2571−2577.
(40) Boys, S. F.; Bernardi, F. *Mol. Phys.* **1970**, *19*, 553.
(41) By a secondary interaction we mean an intramolecular interaction occurring between two (or more) fragments of the same molecule, in which the interacting fragment are covalently linked at a place other than the one where the secondary interaction occurs.

(42) The experimental crystallographic and magnetic data for the new ArFeFeAr and ArCoCoAr compounds will be published in a separate communication: Merill, A.; Nguyen, P.; Sutton, A.; Long, G. J.; Fettinger, J. C.; Power, P. P. Unpublished work, 2007. Some structural parameters for the experimental species are reported in the Supporting Information file.

of each system. Inspection of Table 1 shows that the M−M bond distance is about 1.75–1.85 Å in the M = Cr compounds, while it is ca. 0.1–0.2 Å longer (1.94–1.99 Å) in all the M = Fe and M = Co compounds. For all the MeMMMe systems, the energy as a function of the C−M−M−C dihedral angle was determined in order to test if the structure with a nonplanar C−M−M−C moiety had a lower energy. The results indicate that the energy increases upon closure of the dihedral angle and the planar trans-bent structure exhibits the lowest energy. For MeCoCoMe the possible existence of lower energy minima at a longer Co−Co bond distance (2.80 Å) was also investigated, but the present calculations indicate that there is no such double minimum. The Cr−Cr distance is shorter in the Ph compound than in the Me compound. The other difference between the two species is the CCrCr angle, which is smaller in the Me case rather than in the Ph case. In the Me case a diamond-like structure, in which the two Me are bridging between the two Cr atoms, is the one energetically preferred. This explains why the Cr−Cr bond is longer in the Me compound. The Ph compound, on the other hand, has a more trans-bent-like structure with the PhCrCr angle closer to 90°, and this explains why the Cr−Cr bond is shorter in this case.

The nature of the metal−metal interaction has been analyzed along the Me and Ph series in terms of the metal−metal effective bond order (EBO).[4] The EBOs are reported together with the M−M and C−M bond distances and the dissociation energies in Table 1. For MeCrCrMe, with a Cr−Cr bond distance of 1.849 Å, the following occupation numbers for the natural orbitals involved in the Cr−Cr bond were obtained: σ_g (1.55), σ_u (0.45), π_u (3.04), π_g (0.96), δ_g (3.36), δ_u (0.633). These values yield an EBO of 2.96. A similar study on PhCrCrPh[7] predicted a ^1A_g ground state, with a Cr−Cr bond distance of 1.752 Å for the trans-bent structure. The EBO between the two Cr atoms in that case was calculated to be equal to 3.52. The Cr−Cr bond is significantly longer and weaker in MeCrCrMe than it is in PhCrCrPh, probably because of a stronger interaction between Cr and Me than that between Cr and Ph. Inspection of the molecular orbitals involved in the Cr−Cr bond in the two systems shows that they are more delocalized toward the Cr−C fragment in case of the Me ligand, in comparison to the Ph ligand.

Single point CASPT2 energy calculations were also performed on the Ar′CrCrAr′ coordinates extracted from the X-ray crystallographic structure corresponding to a Cr−Cr bond distance of 1.836 Å. The following occupation numbers for the natural orbitals involved in the Cr−Cr bond were obtained: σ_g (1.64), σ_u (0.35), π_u (3.26), π_g (0.73), δ_g (3.52), δ_u (0.48). These values yield to an EBO of 3.43. In other words, the Cr−Cr EBO and bond distance are similar in the Ar′CrCrAr′ system and PhCrCrPh model compound and little changes occur with respect to the other model compound, MeCrCrMe.

The bonding is vastly different in the Co−Co case. The Co−Co bond distances are 1.95 and 1.94 Å for MeCoCoMe and PhCoCoPh, respectively, which are ca. 0.2 Å longer than the metal−metal distance for the corresponding Cr species despite the smaller size of Co. It was not possible to calculate the EBO value between the two Co atoms in the case of MeCoCoMe, because the orbitals involved in the bonds are highly delocalized over the system. In PhCoCoPh the molecular orbitals are more localized and they yield a much lower EBO of 1.38 for the Co−Co bond. In the Ar′CoCoAr′ case, the Co−Co bond distance greatly increased to 2.80 Å, almost 1 Å longer than it is in the methyl- or phenyl-substituted compounds.

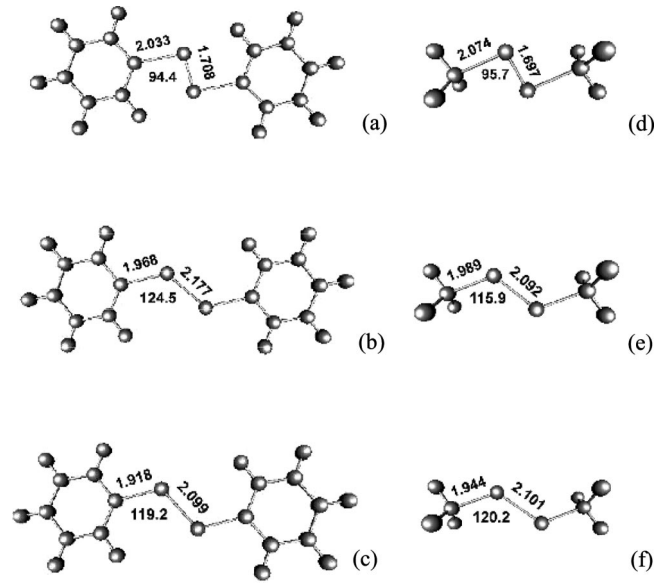

Figure 1. DFT optimized structures of the MeMMMe and PhMMPh species in their ground states obtained at BLYP/ZORA/TZP level. PhMMPh: (a) M =Cr, (b) M = Fe, (c) M = Co. MeMMMe: (d) M =Cr, (e) M = Fe, (f) M = Co.

Table 2. M−M Bond Distances (Å), C−M−M and C−M−M−C angles (deg) in the DFT-optimized Ground States Planar Trans-Bent Structures of MeMMMe and PhMMPh Species at BLYP/ZORA/TZP Level (M = Cr, Fe, Co)[a]

model species (multiplicity)	M−M (Å)	C−M (Å)	C−M−M (deg)
MeCrCrMe, C_{2h} (1)	1.697 (1.626)	2.074 (2.064)	95.7 (92.0)
MeCrCrMe, C_{2h}' (1)	1.695 (1.626)	2.081 (2.078)	99.1 (95.6)
PhCrCrPh, C_{2h} (1)	1.708 (1.634)	2.033 (2.042)	94.4 (93.1)
MeFeFeMe, C_{2h} (7)	2.092 (2.077)	1.989 (1.977)	115.9 (119.5)
MeFeFeMe, C_{2h}' (7)	2.097 (2.070)	1.986 (1.980)	115.4 (121.3)
PhFeFePh, C_{2h} (7)	2.177 (2.173)	1.968 (1.969)	124.5 (124.6)
MeCoCoMe, C_{2h} (5)	2.101 (2.237)	1.944 (1.951)	120.2 (127.4)
MeCoCoMe, C_{2h}' (5)	2.099 (2.227)	1.953 (1.935)	119.9 (124.7)
PhCoCoPh, C_{2h} (5)	2.099 (2.137)	1.918 (1.916)	119.2 (118.1)

[a] Values in parentheses were obtained at B3LYP/pVDZ level.

Analysis of the molecular orbitals shows that the two Co atoms interact exclusively with the flanking arenes and not with each other. The EBO between the two Co is zero in this case. The bonding for the Fe molecules resembles that of their Co counterparts rather than their Cr analogues. For MeFeFeMe, as for MeCoCoMe, it was not possible to calculate the Fe−Fe EBO because of the strong delocalization. To summarize, the CASPT2 results clearly show that the metal−metal interaction is barely affected by the nature of the ligand in the Cr case. On the other hand, it is seriously affected in the Fe and Co case.

For simplicity, only computational results obtained at the quasi-relativistic BLYP/ZORA/TZP level are discussed in the following sections, because the differences in computed geometries between B3LYP/ZORA/TZP and B3LYP/pVDZ are only of minor importance and both approaches exhibit exactly the same trends. However, the reader can find the analogous information from the nonrelativistic calculations in all the tables containing the relevant geometrical parameters. The DFT optimized geometries of the same MeMMMe models in the constrained C_{2h}' symmetry are shown in Figure 1 and the important structural parameters are reported in Table 2. The MeCrCrMe was optimized in the singlet ground state; for the MeFeFeMe and MeCoCoMe the septet and quintet ground

states, as predicted by CASPT2, were used respectively in the calculations. First, the DFT calculated chromium−chromium distances for both C_{2h} and C_{2h}' symmetries (1.697; 1.695 Å) lie in the range of the previously reported Cr−Cr distances that we have obtained probing various combinations of basis sets and functionals.[1] In the optimized MeCrCrMe models, the CrCrC angle is close to 100° (95.7; 99.1°). Not surprisingly, the optimized geometries are very different in the case of the analogous iron and cobalt species: For the Fe species, the optimized MeMMMe structure is characterized by longer metal−metal distances (2.092; 2.097 Å) and a wider FeFeC angle (115.9; 115.4°). The MeCoCoMe species have the longest metal−metal separation with the CoCo distances 2.101 and 2.099 Å, and also the most open CoCoC angle (120.2; 119.9°). The situation is similar for the PhMMPh species. The metal−metal separations are close to 1.7 Å for PhCrCrPh and exceed 2.1 and 2.0 Å in PhFeFePh and PhCoCoPh, respectively. It is worth noting, that none of the optimized planar trans-bent structures, except for the C_{2h}' MeFeFeMe, is a minimum on the potential energy surface (PES). The optimized C_{2h} and C_{2h}' MeCrCrMe models are characterized by one or two negative frequencies, respectively. All the optimized PhMMPh species exhibit two negative frequencies. We have also explored the other possible geometries for the MeMMMe models (see Supporting Information file and the PES scan section of the paper for the characterization of the linear cis-bent and "dangler" MeMMMe geometries), but these are not relevant for the experimental planar trans-bent structures and are not discussed here.

As mentioned in the introduction, DFT yields inappropriate bond lengths for the RCrCrR dimer because of its intrinsic inability to properly treat its multiconfigurational character.[7] The same issue arises in the CoCo and FeFe species, although one would expect the errors to be smaller because of the lower extent of the multiconfigurational character and quantitatively smaller number of d electrons involved in the metal−metal bonding. It is clear however from the DFT optimized geometries that the computed bond lengths for CoCo and FeFe species are much longer (by ~0.4 Å) than those in the chromium analogue. The effect of the substitution of the methyl group by an electron-rich π system such as a phenyl ligand on the metal−metal bonding, is only moderately embraced by DFT since differences in the optimized metal−metal bond lengths of model RMMR species bearing the two ligands are not very significant. These differences are slightly greater in the case of Fe, but are insignificant for Co. However, they remain small compared to the multireference CASPT2 results.

The relaxed potential-energy curves were generated by performing the C_2 constrained optimizations at discrete values of the CMMC torsion angle θ for the high spin configurations of MeFeFeMe and MeCoCoMe dimers (Figure 2) and the singlet spin state MeCrCrMe; analogous curves were obtained for the planar trans-bent geometries where the C−M−M angle φ was varied in the C_{2h} constrained geometry optimizations (see Supporting Information file for details). The PES of the MeCrCrMe model proved particularly complex. The constrained C_2 optimizations were unsuccessful, since for all the geometries with $\theta < 120$, the optimizations led to linear D_{3d} structures, indicating a fairly flat PES in this region. As reported in our previous publications,[1,7] the planar trans-bent geometry scan (Figure S17 in Supporting Information file), where φ is varied, indicates an important barrier (ca. 18 kcal mol^{-1}) around 130° between the trans-bent and the linear structure (similar value

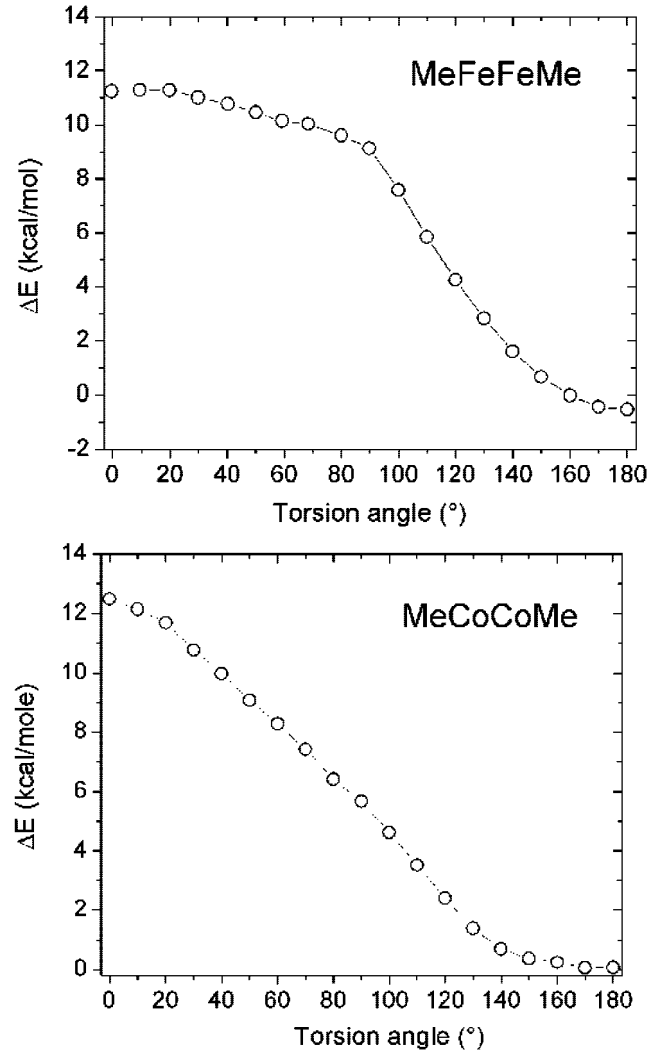

Figure 2. Relaxed torsional angle energy scans for MeMMMe species (M = Fe, Co) obtained at BLYP/ZORA/TZP level of theory.

of 131° and 20 kcal mol^{-1} was found in our previous study of the PhCrCrPh dimer).[7] A rigorous analysis of the potential energy surface for the RCrCrR molecules is currently underway. The computed energy values for the MeFeFeMe and MeCoCoMe C_2 constrained optimizations exhibit monotonically decreasing behavior for the complete 180° rotation around the metal−metal bond with minimum energy for the linear species. In the case of the MeCoCoMe molecule however, the energy values for the torsional angles at 160, 170, and at 180° are almost identical. This part of the curve (torsion angle 160–180°) is very flat, and there is the possibility that a minimum occurs at θ value close to 160°. Nevertheless, a very small energy difference ($\Delta E = 0.2$ kcal mol^{-1}) between this geometry and the planar trans-bent configuration ($\theta = 180°$) makes it rather unlikely. Moreover, the CASPT2 results seem to indicate that the only minimum occurs for the linear species. Finally, the planar trans-bent geometry scans are characterized by minima occurring for the trans-bent MeMMMe species at 110° and 120°, for M = Co and M = Fe, respectively.

Since the electronic structure of the MeCrCrMe was discussed in details elsewhere,[6,43] we present only the bonding picture

(43) Merino, G.; Donald, K. J.; D'Acchioli, J. S.; Hoffmann, R. *J. Am. Chem. Soc.* **2007**, *129*, 15295–15302.

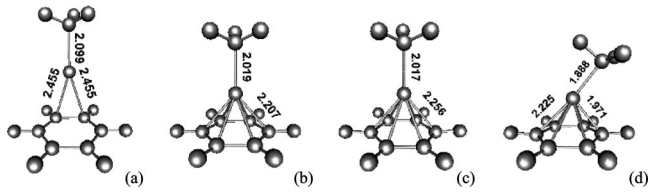

Figure 3. DFT-optimized structures of the MeM−C_6H_6 model species: (a) M =Cr, sextet; (b) M = Fe, quartet; (c) M = Co, triplet; (d) M = Co, singlet. Detailed geometrical parameters are reported in Table 3.

arising from the analysis of the molecular Kohn–Sham orbitals for the planar trans-bent MeFeFeMe and MeCoCoMe species. Briefly, in contrast to the singlet MeCrCrMe analogue where all the five 3d orbitals participate in bonding combinations yielding two π, two σ, and one δ bond for CrCr, in the high-spin septet MeFeFeMe, metal−metal bond is composed of two π bonds that are formed by pairs of metal d_{xz} and d_{yz} orbitals and an additional σ bond, which arises from the combination of d_z^2 orbitals. In the high spin quintet MeCoCoMe, the M−M bond is essentially composed of two d_{xz} orbitals that combine to yield a single π bond and two d_z^2 orbitals, which form an additional σ bond. Details of the Kohn–Sham orbitals for both species are reported in the Supporting Information file.

DFT and CASPT2 Optimized Structures of the Monomeric MeM-C_6H_6 Species. In the first stage of the evaluation of the metal−arene interactions in ArMMAr species, we attempted to optimize the geometries of the monomeric MeM−C_6H_6 models. The optimizations were performed for different spin states in order to assess the tendency to spin pairing of the metal d orbitals that could be potentially induced by the vicinity of the aryl π system. The optimized structures are summarized in Figure 3 (see Table 3 for important geometrical parameters). It is clear that the high-spin states always exhibit the lowest energy for all the three benzene-transition metal monomers. The energy differences between the ground and the next higher energy spin state of lower multiplicity are quite similar for Cr, Fe, and Co, and are ca. 20 kcal mole^{-1}. The most interesting features observed in the optimized structures are the differences in the way the MeM fragment interacts with the benzene ring in the case of the high-spin species. For both Fe and Co, the optimized structures have a η^6 coordination mode and retain the approximate D_{3d} symmetry (no constraints on symmetry were applied during optimizations) with the C_{Me}−M bond being perpendicular to the plane containing the benzene unit, and collinear with the C_6 symmetry axis of the ring. None of these structures however is a minimum on PES and attempts to locate such a minimum remained unsuccessful. In contrast, for chromium, the optimized geometry of the high-spin species, which is a minimum on PES, clearly shows a displacement of the MeM fragment toward a pseudo-η^2 coordination mode (Figure 3), where the C_{Me}−M bond lies on a normal to the ring plane and bisects one of the C−C bonds of the benzene. There are also noticeable differences in the M−C distances to the closest C carbon in benzene, between the Cr and Fe and Co species. These distances, which remain at 2.207 Å (M−centroid = 1.728 Å) and 2.256 Å (M−centroid = 1.807 Å) for Fe and Co, respectively, are much shorter than the corresponding distance for the chromium analogue, for which the distance to the closest two carbons is 2.455 Å (M−centroid = 2.726 Å).

For the lower-spin states the situation is more complex. We encountered severe SCF convergence problems for the lowest

Table 3. Important Structural Parameters for the DFT Optimized (BLYP/TZP/ZORA) MeCr-C_6H_6, (MeMMMe)(C_6H_6,)$_2$, PhMMPh, and Ar$^{\#}$MMAr$^{\#}$ Species in Their Ground States (Bond Distances (Å), Angles (deg))

model	MeCr−C_6H_6	MeFe−C_6H_6	MeCo−C_6H_6 [a]	(MeCrCrMe)(C_6H_6)$_2$ [a]	(MeFeFeMe)(C_6H_6)$_2$ [a]	(MeCoCoMe)(C_6H_6)$_2$ [a]	(MeCrCrMe)(C_6H_6)$_2$ [b]	(MeFeFeMe)(C_6H_6)$_2$ [b]	(MeCoCoMe)(C_6H_6)$_2$ [b]	Ar§CrAr§	Ar§FeAr§	Ar§CoCoAr§	Ar$^{\#}$CrCrAr$^{\#}$	Ar$^{\#}$FeFeAr$^{\#}$	Ar$^{\#}$CoCoAr$^{\#}$
M−M	-	-	-	1.726	2.740	3.116	1.733 (1.647)	2.663 (2.653)	3.006 (3.038)	1.736	2.216	2.211	1.744	2.215	2.467
M−C_{Me}	2.099 (2.102)	2.019 (2.024)	2.017 (2.029)	2.161	2.088	2.048	2.147 (2.117)	2.067 (2.076)	2.033 (2.032)	2.071[d]	1.980[d]	1.972[d]	2.126[d]	2.020[d]	1.998[d]
MMC	-	-	-	119.3	132.5	122.1	115.4 (115.7)	127.5 (128.2)	117.5 (115.6)	99.3	97.0	96.8	102.9	101.9	102.2
CMMC	-	-	-	180.0	180.0	180.0	180.0	180.0	180.0	180.0	180.0	180.0	180.0	171.7	169.2
M−C_1[c]	2.455 (2.475)	2.207 (2.203)	2.256 (2.244)	2.235	2.400	2.188	2.233 (2.230)	2.347 (2.364)	2.219 (2.198)	2.356	2.318	2.189	2.349	2.346	2.210
M−C_2[c]	2.455 (2.475)	2.207 (2.203)	2.256 (2.242)	2.445	2.406	2.229	2.443 (2.453)	2.367 (2.384)	2.242 (2.224)	2.556	2.505	2.324	2.567	2.587	2.284
M−C_3[c]	3.074 (3.032)	2.207 (2.203)	2.256 (2.242)	2.820	2.418	2.310	2.817 (2.847)	2.407 (2.423)	2.286 (2.275)	3.056	2.986	2.696	3.024	3.013	2.511
M−C_4[c]	3.597 (3.515)	2.208 (2.204)	2.256 (2.244)	2.990	2.424	2.350	2.986 (3.024)	2.427 (2.443)	2.308 (2.300)	3.302	3.231	2.898	3.258	3.216	2.699
M−C_5[c]	3.599 (3.518)	2.208 (2.204)	2.257 (2.245)	2.820	2.418	2.310	2.817 (2.847)	2.407 (2.423)	2.286 (2.275)	3.056	2.986	2.696	3.036	2.987	2.573
M−C_6[c]	3.079 (3.037)	2.208 (2.204)	2.257 (2.245)	2.445	2.406	2.229	2.443 (2.453)	2.367 (2.384)	2.241 (2.224)	2.556	2.505	2.324	2.576	2.577	2.325
M−centroid	2.726 (2.691)	1.728 (1.683)	1.807 (1.743)	2.240	1.968	1.791	2.237 (2.261)	1.937 (1.958)	1.783 (1.765)	2.434	2.255	2.082	2.463	2.431	1.990
Δ_{M-M}							0.038	0.566	0.907	0.028	0.124	0.112	0.041	0.126	0.369
Δ_{C-M-M}							16.3	12.1	−2.4	4.9	−17.2	−20.2	7.1	−11.0	−18.6

[a] Constrained to C_{2h} symmetry. [b] Constrained to C_{2h}' symmetry. [c] M−C_n distances defined such as n = 1 corresponds to the closest carbon and the subsequent numbering is done clockwise in the benzene ring. [d] M−C_{ipso} distance. Data in parentheses obtained at B3LYP/pVDZ level of theory.

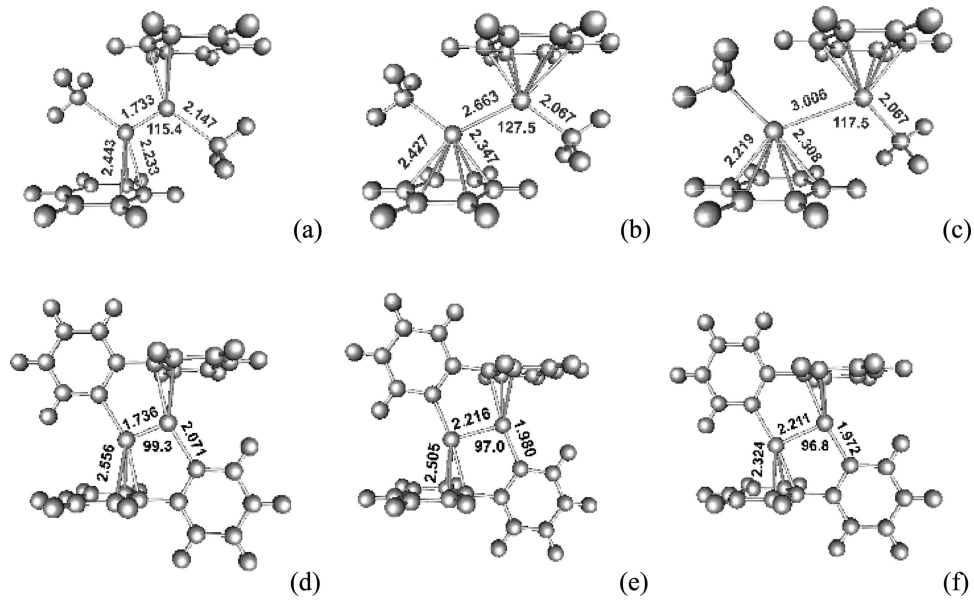

Figure 4. DFT optimized structures of the (MeMMMe)$(C_6H_6)_2$ (a) M =Cr, singlet; (b) M = Fe, septet; (c) M = Co, quintet and $Ar^{\S}MMAr^{\S}$ ($Ar^{\S}$ = C_6H_4-2(C_6H_5)) (d) M =Cr, singlet; (e) M = Fe, septet; (f) M = Co, quintet; model species. Detailed geometrical parameters in Table 3.

spin (doublet) Cr and Fe species and were unable to perform complete optimization geometries of the corresponding molecules. The three small negative frequencies obtained on the partially optimized geometries relate to one rotational and two stretching modes of the methyl fragment. Spurious convergence problems with several transition metals are known, and we are aware of several reports of redundant problems with the geometry optimization problems for several transition metal complexes.[44–46] However, the partially optimized geometries are instructive enough for the purpose of our study. An interesting change in geometry is associated with the spin-state change for MeCo−C_6H_6. The optimized singlet structure exhibits a "bent" geometry with Co-Me bond making an angle of 44.5° with the plane containing the benzene ring. Other details on the low spin monomeric MeM−C_6H_6 species are reported in the Supporting Information file.

The distance between the M−Me fragment and the C_6H_6 ring and their relative positions were reoptimized using CASPT2. In agreement with DFT, CASPT2 predicts a shorter M−C_6H_6 bond distance in $MeFeC_6H_6$ and $MeCoC_6H_6$ than in the $MeCrC_6H_6$ case as well as different bonding mode between these species. For $MeCrC_6H_6$, the M−Me fragment is aligned with one of the C−C bonds of the benzene ring, instead of being centered above C_6H_6. The relevant geometrical parameters of the optimized monomeric species are reported in Supporting Information file.

DFT Optimized Structures of the MeMMMe Models in a Constrained Arene Environment. The optimized structures of the (MeMMMe)$(C_6H_6)_2$ species with the MeMMMe fragment constrained to C_{2h}' symmetry are illustrated in Figure 4 with important geometrical parameters are cited in Table 3. The most striking difference between the CoCo and FeFe models and the corresponding Cr−Cr species is the retention of practically the same M-M distance by the chromium dimer in a constrained conformational space between the two benzene molecules. The optimized geometry (in comparison to the isolated MeCrCrMe species) exhibits only minor changes in the Cr−Cr bond length ($\Delta l_{CrCr} = 0.038$ Å) but is characterized by a significantly wider C−Cr−Cr angle ($\Delta\varphi_{CCrCr} = +16.3°$). This is in contrast to the Fe and Co analogues in which the corresponding MM bond lengths are dramatically affected by the interaction with benzene. The corresponding M-M elongation is 0.566 Å for Fe and it is 0.907 Å for Co respectively. For all the three species the metal–carbon(methyl) bond is very slightly weakened, which is translated into the small elongation of the M-C bonds: $\Delta l_{CCr} = 0.073$, $\Delta l_{CFe} = 0.078$ and $\Delta l_{CCo} = 0.123$.

The change in the CMM angle for Fe is slightly smaller than that found for MeCrCrMe ($\Delta A_{FeFeC} = 12.1°$) but for the MeCoCoMe dimer the angle decreases to an optimized value of 117.5° ($\Delta A_{CCoCo} = -2.4°$). Inspection of the metal-benzene carbon distances in the optimized structures is instructive and shows clearly that for both (MeFeFeMe)$(C_6H_6)_2$ and (MeCoCoMe)$(C_6H_6)_2$, an η^6 coordination mode is adopted. The six M-C (benzene) distances display only a small variation in MeFeFeMe and MeCoCoMe, whereas for the MeCrCrMe species, major asymmetry is apparent and the Cr-benzene coordination can be described as between η^1 and η^3 (depending on how the "coordinating" C-M distance is defined). In the process of optimizing the (MeMMMe)$(C_6H_6)_2$ structures, we have also attempted to lift the C_{2h} symmetry constraint relating the planar MeMMMe fragments to the frozen geometry of the benzene rings. Although these attempts did not afford fully optimized structures due to an oscillatory behavior of the geometry optimization cycle (see Supporting Information file for the partially optimized geometries), it was however interesting to find that in case of the chromium dimer, the planar MeCrCrMe fragments adopts a slightly "twisted" conformation out of the initial symmetry plane containing the CMMC core and 4 out of 12 carbon atoms of the nearby benzenes. In this particular geometry, the plane containing the CCrCrC core of the MeCrCrMe, almost exactly bisects the C−C bond of each

(44) Daniels, A. D.; Scuseria, G. E. *Phys. Chem. Chem. Phys.* **2000**, *2*, 2173–2176.
(45) Rabuck, A. D.; Scuseria, G. E. *J. Chem. Phys.* **1999**, *110*, 695–700.
(46) Wedderburn, K. M.; Bililign, S.; Levy, M.; Gdanitz, R. J. *Chem. Phys.* **2006**, *326*, 600–604.

Table 4. DFT Calculated Wiberg Bond Orders (WBO) on the Optimized Structures of MeM−C_6H_6, (MeMMMe)$(C_6H_6)_2$ model species, and Ar′MMAr′ experimental species[a]

	Cr	Fe	Co
MeMMMe			
M-M	4.94	1.63	1.23
M-C	0.87	0.91	0.97
[b]MeMMMe (LS)*	(HS)		
M-M	0.54	3.49	2.29
M-C	0.78	1.08	1.10
PhMMPh			
M-M	4.77	1.28	1.26
M-C_{ipso}	0.81	0.98	0.99
(MeMMMe)$(C_6H_6)_2$			
M-M	4.22	0.50	0.17
M-C	0.89	0.87	0.88
M-C_6H_6	0.95	1.50	1.96
MeM-C_6H_6			
M-C_{Me}	0.93	0.91	0.95
M-C_6H_6	0.53	2.47	2.04
ArMMAr			
M-M	4.11	0.44	0.10
M-C_{ipso}	0.98	0.73	0.89
M-Ar	0.17	1.23; 1.57	1.90

[a] (a) M = Cr, singlet; (b) M = Fe, septet; (c) M = Co, quintet. [b] Computed for comparison in high spin Cr ($S = 5$) and low spin Fe ($S = 0$) and Co ($S = 0$) species.

of the benzene molecule. This configuration is very similar to the conformation of the MeCr fragment in the optimized structure of the monomeric MeCr-C_6H_6.

DFT Optimized Structures of the Ar§MMAr§ (Ar§ = C_6H_4-2(C_6H_5) and Ar$^{\#}$MMAr$^{\#}$ (Ar$^{\#}$ = C_6H_3-2,6-(C_6H_3-2,6-Me_2)$_2$) Model Species. The important geometrical features of the optimized Ar§MMAr§ and Ar$^{\#}$MMAr$^{\#}$ species are reported in Table 3. The M−M bond lengths in the Ar§CrCrAr§ and Ar$^{\#}$CrCrAr$^{\#}$ are very similar to the ones obtained in the planar trans-bent PhCrCrPh models optimized at the same level of theory. We have previously attributed the small elongation ($\Delta L_{CrCr} = 0.041$ Å) between PhCrCrPh and Ar$^{\#}$CrCrAr$^{\#}$ to the interaction of the Cr atoms with the nearby flanking aryl, and apparently it is also responsible for the small discrepancy between the CASPT2 calculated Cr−Cr distance in PhCrCrPh and the experimental Cr−Cr separation found in the X-ray crystal structure of the Ar′CrCrAr′.[7] The optimized C_{2h} geometries of the Ar§FeFeAr§ and Ar§CoCoAr§ are, as expected, very similar to the Ar$^{\#}$FeFeAr$^{\#}$ and Ar$^{\#}$CoCoAr$^{\#}$ species. However these latter exhibit two important features: first, the C_{ipso}−M−M−C_{ipso} core is not completely planar as in the case of the Ar$^{\#}$CrCrAr$^{\#}$ (171.7 and 169.2°). In addition, all the three geometries are characterized by much narrower C_{ipso}−M−M angles: 102.9, 101.9, and 102.2° for Cr, Fe, and Co, respectively (note that the C_{ipso}−Cr−Cr angle in the experimental structure is 102.8°). The M−M elongations in Ar§MMAr§ and Ar$^{\#}$MMAr$^{\#}$ versus the optimized PhMMPh species for iron and cobalt are smaller than the analogous elongation computed for the MeMMMe/(MeMMMe)$(C_6H_6)_2$ congeners. They remain however significantly longer than in the corresponding ArCrCrAr species (0.028 vs 0.039 and 0.112 Å for Fe and Co, respectively, in Ar§MMAr§) and 0.041 vs 0.126 and 0.369 Å for Fe and Co species, respectively, in Ar$^{\#}$MMAr$^{\#}$.

DFT Calculated Wiberg Bond Orders (WBO). The calculated Wiberg bond orders are compiled in Table 4. First, we report the calculations on the model Ar′MMAr′ (Ar′ = C_6H_3-2,6(C_6H_3-2,6-Pr^i_2)$_2$) molecules on coordinates obtained from the single crystal X-ray analysis. As previously highlighted, the DFT calculation on a singlet chromium dimer results in a Wiberg bond order of 4.11 and is, as expected, less than a value corresponding to a formally quintuple bond. The metal−metal WBOs for Fe and Co are 0.44 and 0.10, respectively, and correspond, at least in case of Co, to an essential absence of bonding between metal centers.

The WBOs calculated for the Cr−Cr dimer in the MeMMMe and PhMMPh models are in agreement with those found in the Ar′CrCrAr′ species. The higher Cr−Cr bond orders (4.94, 4.77) in comparison to the Ar′CrCrAr′ molecules are due to the absence of multiple atomic centers in the surrounding ligands and consequently to a simpler spatial extent of the molecular orbital overlaps. The WBOs for the analogous FeFe and CoCo species are relatively low (1.63, 1.28, and 1.23, 1.26), but this is expected for the high-spin septet and quintet metal−metal interactions.

The bond orders calculated for the arene−metal interactions are also of considerable interest. First, in the "monomeric" MeM−C_6H_6 models, where no metal−metal interaction is present, the calculated bond orders are quite different for Cr, Fe, and Co. The Cr−benzene interaction has a WBO of only 0.53,[47] whereas the corresponding bond orders for benzene−Fe and benzene−Co exceed two (2.47 for Fe and 2.05 for Co). This is indicative of strong covalent interaction between the Me−metal fragment and the π system of benzene. Another important observation is the trend in the WBOs calculated in the constrained arene geometry for the (MeMMMe)$(C_6H_6)_2$ species. The metal−metal bond order for Cr−Cr is moderately diminished (4.22 vs 4.94) but the bond order remains higher than four. In contrast, the already low M−M bond orders for Fe and Co are lowered further: from 1.63 to 0.50 for Fe and from 1.23 to 0.17 for Co. This trend is accompanied by a substantial increase in the metal−benzene BO: 1.50 and 1.96 for FeFe and CoCo, respectively. Finally, the methyl carbon−metal bond orders remain almost unaffected and are essentially independent of the presence (or absence) of the secondary arene−metal interaction.

Interaction Energies. The metal−metal bond energies obtained from the CASPT2 calculations are in agreement with the intuitive trend expected for these metal dimers: 75 kcal mole^{-1} for quintuply bonded PhCrCrPh, followed by 61 kcal mole^{-1} for PhCoCoPh and 36 kcal mole^{-1} for PhFeFePh (Table 1). The interaction energies in the (MeMMMe)$(C_6H_6)_2$ species based on the fragment oriented approach were calculated on the previously optimized structures and are reported in Tables 5 and 6. Note that within the hybrid B3LYP approximation to the exchange-correlation functional, the energy difference corresponding to the bonding energy between the two MeCr fragments in MeCrCrMe remains positive ($\Delta E = +57$ kcal mole^{-1}). The energy values computed at the BLYP/ZORA/TZP level show a very small and positive interaction energy between MeCr and benzene ($\Delta E = +2.5$ kcal mole^{-1}), but this value lies within the limit of the DFT accuracy, and consequently the sign of the energy has to be taken with caution. Nevertheless, it is clear that the calculated MeM−benzene interaction energies are higher for the Fe and Co species (−8.1 and −22.8 kcal mole^{-1}, respectively), in comparison to MeCr−C_6H_6. An approximate estimate of the stabilization energy provided by the

(47) However, thermochemical and computational data show that η^6-C_6H_6-Cr bonding is in the range of ca. 35–40 kcal mol^{-1} in Cr(0) bisarene complexes. See: Skinner, H. A.; Coonor, J. A. *Pure Appl. Chem.* **1985**, *1957*, 1979.

Table 5. The Interaction Energies (kcal mol^{-1}) Calculated at the BLYP/ZORA/TZP Level of Theory Using Fragment-Oriented DFT Approach in the Optimized Structures of (MeMMMe)(C_6H_6)$_2$ Model Species (Values in Parentheses Obtained at B3LYP/pVDZ Level)

	M−M	M′−M′	ΔE_{stab}[a]	MeM−C_6H_6
(MeCrCrMe)(C_6H_6)$_2$	−28.2 (+47.1)	−16.5 (+57.0)	−15.6 (−11.4)	+2.5 (+1.8)
(MeFeFeMe)(C_6H_6)$_2$	−44.6 (−29.1)	−25.1 (−8.6)	−20.5 (17.0)	−8.1 (−3.1)
(MeCoCoMe)(C_6H_6)$_2$	−40.7 (−49.2)	−26.9 (−35.9)	−12.9 (−9.8)	−22.8 (−21.5)

[a] As calculated from difference between the energy of the optimized (MeMMMe)(C_6H_6)$_2$ and the similar optimized structure, where the MeMMMe fragment was restrained to the geometry obtained for the isolated MeMMMe

Table 6. The Interaction Energies (kcal mol^{-1}) Calculated at BLYP/ZORA/TZP Level of Theory Using Fragment-Oriented DFT Approach in the Optimized Structures of MeM−C_6H_6 Model Monomeric Species (Values in Parentheses Obtained at B3LYP/pVDZ Level)

	MeM−C_6H_6
MeCr- C_6H_6	−9.6 (−4.9)
MeFe- C_6H_6	−22.9 (−17.1)
MeC- C_6H_6	−22.1 (−27.7)

secondary interaction with benzene can be obtained from the energy difference between the optimized (MeMMMe)(C_6H_6)$_2$ dimer and the similar structure in which the optimization was performed with constraints on the MeMMMe fragment (kept as optimized on the isolated MeMMMe molecule). This energy is similar for Cr and Co species (15.6 and 12.9 kcal mol^{-1}, respectively) and slightly higher for Fe species (−20.5 kcal mol^{-1}).

The interaction energies were also calculated for the optimized monomeric species where the mutual arrangement of the two fragments (MeM vs benzene) is different (Me-M bond perpendicular to the plane of the benzenic ring). Although the computed energies exhibit higher absolute values (note that for MeCr-C_6H_6 the energy is now negative), the overall trend is identical. For the η^2 coordinated MeCr in MeCr-C_6H_6, small interaction energy of −9.6 kcal mole^{-1} is found, while for the η^6 coordinated MeFe-C_6H_6 and MeCo-C_6H_6 the values are almost identical, but much higher: −22.9 and −22.1 kcal mole^{-1} for Fe and Co analogues, respectively.

Discussion

The optimized geometries of the MeMMMe and PhMMPh models calculated with the CASPT2 method show that for M = Cr the metal−metal interaction is significantly affected by the nature of the ligand (Me vs Ph), in particular the CrCr bond length is shortened by ca. 0.097 Å. The corresponding effective M−M bond order (EBO) increases from 2.96 in MeCrCrMe to 3.52 in PhCrCrPh. The latter value is very close to that calculated for the entire Ar′CrCrAr′ molecule (3.43). The CASPT2 calculations show that the nature of the metal−metal bond (although not the metal−metal distances) in the RFeFeR and RCoCoR species is modified by replacement of Me with Ph. For example for the cobalt dimers, although there is only a minor shortening of the Co−Co bond by ca. 0.008 Å, it is accompanied by the reduction of the EBO from 2.72 in MeCoCoMe to 1.38 in PhCoCoPh. Moreover, the analogous calculation performed on Ar′CoCoAr′ results in an EBO of zero. Similar behavior is also observed for the iron species: the FeFe bond is shortened by 0.019 Å, but the EBO is reduced from 2.31 in MeFeFeMe to 1.47 in PhFeFePh.

The DFT calculations performed on the same model species show a slightly different picture. The Wiberg bond orders (WBO) calculated for the optimized MeMMMe and PhMMPh species remain almost unaffected, and the nature of the ligand does not seem to induce any significant change in the computed WBO within the DFT framework. This is an interesting observation, since it not only confirms the known issues intrinsic to the limited ability of DFT to properly describe the metal−metal bonding in these transition metal dimers, but also raises the question of the correctness of the WBOs calculated within the DFT frame for these truly multiconfigurational species.

At this point, it is interesting to recall the electronic structure of the Cr, Fe, and Co dimers. The main difference between the monovalent first series transition metal RMMR species and the analogous M_2 dimers lies in the fact that in the former, a pair of 4s electrons is used to form the M−C bond with the ligand. However, with this exception only, the overall electronic configuration should remain the same. As discussed in our previous paper on the PhCrCrPh, its CrCr $3d\sigma_g^2 3d\pi_u^4 3d\delta_g^4$ + CrC $4s\sigma_g^2$ singlet ground configuration (with all the spin-paired electrons) corresponds to the analogous configuration obtained for Cr_2: $3d\sigma_g^2 3d\pi_u^4 3d\delta_g^4 4s\sigma_g^2$ where the two 4s electrons participate in the metal−metal bonding. A similar situation occurs in RCoCoR and RFeFeR. For RCoCoR, CASPT2 yields the quintet ground state (^5B_u in the MeCoCoMe case, and ^5B_g in the PhCoCoPh case) which has its homologue in the quintet ground-state configuration of Co_2 obtained by DFT calculations:[48] $[3d\sigma_g^1 3d\pi_u^2 3d\delta_g^2 4s\sigma_g^1 3d\sigma^{*1}_u 3d\pi^{*2}_g 3d\delta^{*2}_u]\uparrow[3d\sigma_g^1 3d\pi_u^2 3d\delta_g^2 4s\sigma_g^1 3d\delta^{*1}_u]\downarrow$. In the case of RFeFeR (R = Me and Ph) with the ^7A_u septet, the corresponding ground state for Fe_2 is expressed as $[3d\sigma_g^1 3d\pi_u^2 3d\delta_g^2 4s\sigma_g^1 3d\sigma^{*1}_u 3d\pi^{*2}_g 3d\delta^{*2}_u]\uparrow[3d\sigma_g^1 3d\pi_u^2 3d\delta_g^1 4s\sigma_g^1]\downarrow$.

With these data in hand, it is worthwhile to examine the factors involved in the rather dramatic differences between (a) the chromium dimer, where the secondary ligand interactions have only a minor effect on the geometry of the CMMC core as well as the quintuple character of the Cr−Cr bond and (b) the Co and Fe species, where analogous interactions result in an almost complete disruption of the bonding between the metal centers in the computed ArMMAr and (MeMMMe)(C_6H_6)$_2$ structures. The first point of concern is the interaction of the monomeric MeM fragment with benzene. From the results obtained on the monomeric MeM-C_6H_6 species it is obvious that the interaction of the MeCr fragment is very much weaker than those observed for MeFe and MeCo. In the chromium case, the preferred geometry (see Figure 3) is an approximately η^2 bonding mode, while an η^6 coordination mode is observed for Fe and Co. The differences are also confirmed by the inspection of the corresponding bonding energies. The interaction energy between the MeCr fragment and C_6H_6 is relatively small (or even positive when the MeCr fragment is "bent" toward C_6H_6), while the analogous bonding interactions for Fe and Co exceed 20 kcal/mol). The large difference between the

(48) Gutsev, G. L.; Bauschlicher, C. W. *J. Phys. Chem. A* **2003**, *107*, 4755–4767.

strength of the interaction of benzene with the MeCr moiety and its interaction with the MeFe and MeCo fragments is perhaps the most striking feature of the computational results. What are the reasons for such different complexation behavior? The origins of the different interaction energies are not straightforward. Simple electronic considerations suggest that the Cr−benzene interactions should be the strongest, since the valence electron count of MeCr (7) is lower than MeFe (9) and MeCo (10), and hence it should bind more strongly to the benzene π-electrons. This is not the case, however, and other factors are apparently of greater importance. One possible contributing factor to the weakness of the MeCr−benzene interaction is the d^5-electron configuration of the MeCr moiety. The d^5 configuration has a favorable exchange energy which is lost if there is a strong η^6-π-interaction with an aryl ring. Our calculations clearly show that the high-spin d^5 configuration is preserved in the weak MeCr(η^2-C_6H_6) complex, and the average energy of the d^5 levels increases slightly. In addition, the HOMO e_1 levels of the benzene are only slightly stabilized upon complexation. In contrast, both the metal d-electrons and the benzene π-levels in the iron and cobalt complexes become stabilized, consistent with the formation of a stronger complex with the C_6H_6 ring. Another possible factor relates to the ionic size of the metal centers. Chromium is the largest of the three metals and in purely electrostatic terms is expected to have the weakest interaction with π-electrons of the aryl ring. Although these reasons seem plausible, they have not been quantified to date. Perhaps the most surprising aspect of these results is the fact that the weakness of the interaction between an arene and a monohapto ligated d^5 metal fragment had not been anticipated. This is especially so in light of the extremely large volume of experimental and theoretical work in the metal−arene area. The very similar Cr−C_6H_6 bonding energies found in the monomeric MeCr−C_6H_6 and dimeric (MeMMMe)(C_6H_6)$_2$ species strongly suggests that the inability of a high-spin monodentate RCr(I) fragment to strongly complex an arene partner is an inherent property of this high-spin moiety.

Additional conclusions can also be drawn from the analysis of the Wiberg bond orders for the (MeMMMe)(C_6H_6)$_2$ species, which reflect the ability of the secondary metal−arene interaction to disrupt the metal−metal bonding. It is noteworthy that instead of relatively short CoCo and FeFe bonds predicted by both DFT and CASPT2 calculations for MeMMMe and PhMMPh, an almost complete absence of M−M bonding has been observed experimentally in Ar′MMAr′ (M = Fe or Co)[42] which display strong η^6-metal−arene interactions to the flanking aryl rings. This is in agreement with the computations for the model (MeMMMe)(C_6H_6)$_2$ species. The decrease of WBOs for the M−M bond from 1.63 in MeFeFeMe (1.28 in PhFeFePh) to 0.53 in (PhFeFePh)(C_6H_6)$_2$ or even to 0.44 in the experimental ArFeFeAr, does not leave any doubt that there are two formally unbound metal fragments that are in effect "half-sandwich" moieties. The same situation occurs in case of Co, where the similar decrease in WBO is even more striking: from 1.23 in MeCoCoMe to 0.18 in (MeCoCoMe)(C_6H_6)$_2$ and 0.10 in ArCoCoAr. These results are reinforced by the CASPT2 calculations. The EBO calculated for ArCoCoAr is formally zero.

Before summarizing our final conclusions, it is important to restate some issues that are intrinsic to the model used in this study. First, since the terphenyl ligands are characterized by a large flexibility, one can legitimately argue that the metal−metal separation could only be dictated by the metal−metal interaction itself and that the secondary interaction with the flanking aryl is just a *post factum* occurrence, due to the specific spatial extent of the ligand. However, proving this computationally is not a simple matter as we have seen. Thus, the choice of the C_6H_6−C_6H_6 separation in our (MeMMMe)(C_6H_6)$_2$ models (distances taken from the experimental structures) may seem a little arbitrary. However, in order to obtain insight into the energetics of the M−C_6H_6 interactions and related structural changes, one has to proceed with the fragmentation (i.e., "division" into separate halves) of the molecular system under investigation. Such fragmentation automatically induces a certain lack of control of the interacting fragments, and this is the main reason for the choice of the frozen constrained benzene environment imposed in our model, which is, of course, based on the actual experimental findings. This begs the question of how different would the interaction of the metal center with flanking aryl be in comparison to the M−C_6H_6 interaction in our simplified model? Even if such interactions were different (there are no good reasons to expect large differences), it is difficult to model the flanking aryl−metal interaction without disconnecting it from the central ligand ring bearing the metal center. It is noteworthy that the results obtained with the optimized geometries of the "connected" ligands, modeled using Ar§MMAr§ or even more crowded Ar$^{\#}$MMAr$^{\#}$ species, show exactly the same trend as in the (MeMMMe)(C_6H_6)$_2$, even though there are large size and flexibility differences between the ligands present in both these model species.

Conclusions

Calculations performed on a simple molecular model to probe the extent of feeble arene−metal interactions that occur in the transition metal dimers bearing the terphenyl ligands suggest that at least two factors contribute to the structural differences observed between the quintuply bonded chromium dimer and its cobalt and iron congeners. First, the robustness of the Cr−Cr quintuple bond is related to the character of the RCr(I) species, whose electronic (d^5) structure precludes strong interactions with the nearby arenes, such as benzene or phenyl fragments. This apparent reluctance to interact more strongly with the surrounding π system of the ligand is an important factor that contributes to the stability of the quintuple Cr−Cr bond. The most important attribute of the CrCr bond is the presence of a high number (10) of valence electrons that exactly match the number of bonding molecular orbitals. It is noteworthy that the recently synthesized monomeric, univalent chromium(I) compounds 3,5-Pr^i_2Ar*CrL (3,5-Pr^i_2Ar* = C$_6$H-2,6(C_6H_2-2,4,6-Pr^i_3)$_2$-3,5-Pr^i_2, L = THF or PMe_3) whose crystal structures reveal either a THF or a PMe_3 molecule coordinated to two coordinate chromium, decompose when reacted with toluene or benzene.[49] In contrast, the analogous Fe or Co derivatives form stable η^6 complexes with arenes to the exclusion of metal−metal bonding.[50] Further design and tuning of the ligand should allow unwanted, "spurious" metal–ligand interactions to be excluded. In addition, the significant differences in the occupations of the bonding and antibonding

(49) Wolf, R.; Brynda, M.; Ni, C.; Long, G. J.; Power, P. P. *J. Am. Chem. Soc.* **2007**, *129*, 6076–6077.
(50) Ni, C.; Ellis, B. D.; Fettinger, J. C.; Long, G. J.; Power, P. P. *Chem. Commun.* **2008**, 1014.

parts of the frontier orbitals observed in the CASPT2 calculations for Me and Ph ligands (which in case of Fe and Co result in a quite different metal−metal bond orders), suggests that in contrast to the Cr dimer, new ligands with strong electron acceptor or electron donor groups could be designed to influence the nature of the metal−metal interaction in these low-valent transition metal dimers.

Acknowledgment. We acknowledge the National Science Foundation for partial financial support. G.L.M. and L.G. thank the Swiss National Science Foundation Grant No. 20021-111645/1. M.B. acknowledges the use of the computational resources at the University of Geneva.

Supporting Information Available: Complete ref 38, Cartesian coordinates of the optimized model species, details of PES scans, and details of the DFT calculations. This material is available free of charge via the Internet at http://pubs.acs.org.

JA0771890